

ARTICLES

Field-Optimized Initial State-Based Selective Control of IBr Photodissociation

Deepa B. Bairagi,^{†,‡} Peter Gross,[§] and Manoj K. Mishra^{*,†}

Department of Chemistry, Indian Institute of Technology, Powai, Bombay 400 076, India, and Tata Institute of Fundamental Research, Homi Bhabha Road, Bombay 400 005, India

Received: May 30, 1996; In Final Form: November 11, 1996[⊗]

A new scheme for controlling photodissociation through preparation of a variationally optimized linear superposition of field-free vibrational eigenstates is applied for selective control of IBr photodissociation. The dependence of IBr photodissociation on various field parameters and initial conditions is explored. In a broad range of field parameters, the product yield is shown to increase considerably when a photolysis pulse is applied to the variationally optimized linear combination as opposed to photolysis of IBr with the entire population in a single vibrational level. The frequency, intensity, and phase dependence of this enhancement is explored for both CW and Gaussian pulses.

I. Introduction

The control of photodissociation of simple molecules has received considerable theoretical and experimental attention in the past decade, and rapid developments in laser technology and computational power have fueled an explosion of research in this area. Most of these approaches to control veer around the dream of utilizing lasers as molecular scissors^{1–3} and are focussed on the design of an appropriate laser field to achieve the desired photodissociation objective. The different established theoretical approaches to control have been reviewed recently,^{4,5} and these approaches based on field-induced control have been either perturbative^{4–8} and hence of somewhat limited utility or have provided fields with undesirable attributes like very high intensity⁹ and require computationally demanding procedures for their specification.^{9–11} A more generalized approach to molecular control has been proposed recently.¹² While the focus of these theoretical approaches has been on field design, the photodissociation yield has also been found to be extremely dependent on the choice of initial vibrational state from which photolysis is induced, and results for HI,^{13–15} HCl,¹⁶

and HOD¹⁷ reveal a crucial role for the initial condition of the system in product selectivity and enhancement.

This critical dependence on initial vibrational state indicates that a suitably optimized linear superposition of the initial vibrational levels may be another route to selective control of photodissociation. In any case, since in the field design-based control high intensity is undesirable, phase dependence has been found to be weak,⁸ and considerable success has been demonstrated using a single carrier frequency, it seems desirable to choose a well motivated field to induce photolysis and focus on achieving selectivity and control through optimization of the linear superposition of vibrational states for enhanced photodissociation out of the desired channel.

Recently we have proposed a simple Rayleigh–Ritz variational optimization procedure¹³ for obtaining the optimal linear superposition of the field-free vibrational eigenstates that would lead to flux maximization out of the desired channel for a given photodissociation pulse. This approach to control shifts the focus from control via field design to control via design of an optimal initial state for the chosen field and is computationally simple to implement. The initial demonstrative application to the HI photodissociation has shown a marked enhancement in selectivity and product yield using these field-optimized initial states.¹³ It is interesting to note that the method proposed here is similar to the pump and dump scheme analyzed by Tannor

[†] Indian Institute of Technology.

[‡] CSIR Research Fellow.

[§] Tata Institute of Fundamental Research.

[⊗] Abstract published in *Advance ACS Abstracts*, January 1, 1997.

and Rice⁶ with the role of excited state in their approach from which the wavepacket was dumped using an optimal dump pulse for the given pump pulse being reversed here, where we are optimizing the initial state for the chosen pump pulse.

The photofragmentation spectroscopy of IBr has been studied widely,¹⁹ and it has served as the molecule of choice for some earlier theoretical investigations of controlled photodissociation.^{20,21} In this paper, we apply the field-optimized initial state-based control of IBr for a variety of fields to establish a correlation between field parameters and the enhancement in the selectivity/yield achieved by this new approach. This should help elicit general insights for active photodynamic control of photodissociation products.

The remaining part of this paper is organized as follows. Section II briefly outlines the methodology adopted for establishing the optimal initial condition required for flux maximization out of the desired channel. In section III we present a detailed appraisal of the field dependence of IBr photodissociation and the initial states which will maximize it for both CW and Gaussian pulses. Some concluding remarks are offered in section IV.

II. Method

For molecules possessing a dipole moment $\vec{\mu}$, the effect of the radiation field $\vec{\epsilon}(t)$ may be obtained by solving the time dependent Schrödinger equation (TDSE),

$$i\hbar \frac{\partial \psi}{\partial t} = \hat{H}(t)\psi \quad (1)$$

where,

$$\hat{H}(t) = \hat{H}_0 + \vec{\mu} \cdot \vec{\epsilon}(t)$$

with H_0 being the field-free Hamiltonian. The solution ψ at some time T can be expressed as

$$\psi(T) = \hat{U}(T,0)\psi(0) \quad (2)$$

where $\hat{U}(T,0)$ is the (not necessarily unitary) propagator, and $\psi(0)$ is the wavefunction for the initial state of the molecule to which the photodissociation pulse $\vec{\epsilon}(t)$ is applied. Defining the time-integrated flux operator \hat{F} as

$$\hat{F} = \int_0^T dt \hat{U}^\dagger(t,0) \hat{j} \hat{U}(t,0) \quad (3)$$

where

$$\hat{j} = \frac{1}{2m} [\hat{p} \delta(r - r_d) + \delta(r - r_d) \hat{p}] \quad (4)$$

with m as the reduced mass, \hat{p} the momentum operator along the reaction coordinate, and r_d the grid point in the asymptotic region where the flux is evaluated. Note that in the case of more than one possible dissociation channel, the operator \hat{j} is channel specific, and in a discrete representation of the electronic curves on a spatial grid, r_d denotes the grid point appropriate to the desired channel. The time-integrated flux, which is directly related to the product yield, is

$$\int_0^T dt \langle \hat{j} \rangle_t = \int_0^T dt \langle \psi(t) | \hat{j} | \psi(t) \rangle \int_0^T dt \langle \psi(0) | \hat{U}^\dagger(t,0) \hat{j} \hat{U}(t,0) | \psi(0) \rangle \quad (5)$$

or

$$\int_0^T dt \langle \hat{j} \rangle_t = \langle \psi(0) | \hat{F} | \psi(0) \rangle \quad (6)$$

and it is clear from the above equation that the product yield may be controlled by both altering the field dependent part \hat{F} or the field free initial state $\psi(0)$. Earlier control schemes^{4–12} have attempted control over photodissociation entirely through field manipulation for a fixed $\psi(0)$. Recently we have proposed a scheme where control over product yields is sought through preparation of the initial wave function $\psi(0)$ as a coherent superposition of vibrational eigenstates of the ground electronic potential for the chosen photolysis pulse.¹³ For the short femtosecond pulses to be considered here, rotational motion is ignored. Of course, the field itself may also be altered which will change the nature of the optimal $\psi(0)$.

By expanding $\psi(0)$ in a basis of $(M + 1)$ field-free vibrational eigenfunctions

$$\psi(0) = \sum_{m=0}^M c_m \phi_m \quad (7)$$

flux maximization is reduced to the familiar Raleigh–Ritz variational optimization of $\{c_m\}$ through diagonalization of an $(M + 1 \times M + 1)$ matrix \mathbf{F} whose elements

$$F_{kl} = \langle \phi_k | \hat{F} | \phi_l \rangle \approx \Delta t \sum_{n=0}^{N_t} \langle \psi_k(n\Delta t) | \hat{j} | \psi_l(n\Delta t) \rangle \quad (8)$$

with Δt as the step size for the numerical time propagation and $N_t \Delta t = T$.

The largest eigenvalue f_{\max} of \mathbf{F} is the maximum product yield (flux), and the corresponding eigenvector $\{c_m^{\max}\}$ is the set of coefficients which defines the optimal initial wave function

$$\psi^{\max}(0) = \sum_{m=0}^M c_m^{\max} \phi_m \quad (9)$$

constituting the superposition that will provide the maximum achievable product yield f_{\max} out of the particular channel specified by \hat{F} for the chosen field $\vec{\epsilon}(t)$. As in other similar calculations, the larger the basis set size the “better” the results. However, due to the difficulties in the simultaneous overtone excitation of many vibrational levels, the basis set expansion in eq 7 is restricted to only the first few vibrational eigenstates (only the ground plus the first two excited vibrational levels in our case), and so the size of the \mathbf{F} matrix is small and therefore computationally trivial to diagonalize.

The results to be presented here are from modeling of the IBr molecule as a rotationless oscillator. For the ultrashort pulses employed here, the neglect of rotational effects may be taken to be permissible, since a recent *ab initio* investigation of the photofragmentation of HCl²² has shown negligible influence of molecular rotation on the branching ratio. In any case treatment of rotational effects will greatly influence the computational complexities, and we have therefore found it judicious to neglect rotational motion in this initial application.

The solution proceeds by propagating the TDSE $M + 1$ times from $t = 0$ to $t = T$ for each initial condition $\psi(0) = \phi_m$, $m = 0, 1, \dots, M$. The field-free eigenstates ϕ_m are obtained using the Fourier Grid Hamiltonian method.²³ During propagation the matrix elements \mathbf{F}_{kl} , are accumulated according to eq 8 as has been described in detail elsewhere.¹³

In this paper we attempt a detailed investigation of the selectivity and product enhancement in IBr photodissociation using this new approach. For the ultrashort photolysis pulses

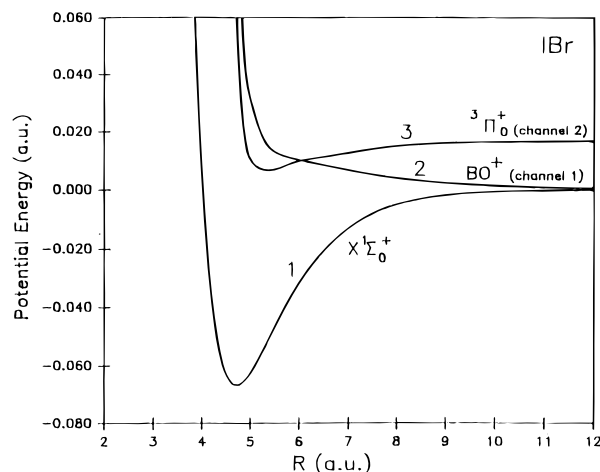


Figure 1. Potential energy curves of IBr.

considered here, IBr has been modeled as a rotationless oscillator, and the three potential energy curves are given in Figure 1. The transition dipole moments used here are the same as those employed earlier.²¹ The energies of the vibrational eigenstates of the ground potential energy curve were evaluated using the Fourier Grid Hamiltonian method,²³ and the TDSE was numerically solved using the Split Operator Fast Fourier Transform (SOFFT) method^{24,25} incorporating propagation via Pauli matrices.²⁶ The total spatial grid of 10 au starting from 2.0 au was divided into 1024 equally spaced points. The flux was monitored at 10.0 au beyond which a “ramp” type optical barrier of height 0.01 au was set up till the end of the grid to prevent any unphysical reflection of the wavepacket. The flux out of the channel 1 (J_1) corresponds to the products $I + \text{Br}(^2P_{3/2})$ (state 1 and 2) and J_2 denotes flux out of the excited $I + \text{Br}^*(^2P_{1/2})$ (the Π_0^+ state labeled 3 in Figure 1) product channel. The analysis to be presented here is for the multicolor CW field of the form $\epsilon(t) = A \sum_{p=0}^2 \cos(\omega - \omega_{p,0})t$ where A is the amplitude, ω the photodissociation frequency, and $\omega_{p,0} = (E_p - E_0)/\hbar$ the Bohr frequency for the transition between the p_{th} and the ground 0_{th} vibrational energy levels. Propagation is done for 20000 au (485 fs) with the field on and allowed to propagate further for another 16000 au (390 fs).

III. Results and Discussions

The variation of maximized flux out of channels 1 and 2 as a function of field amplitude at a laser frequency $\omega = 0.089$ au (19533 cm^{-1}) using the optimal combinations ψ_1^{max} and ψ_2^{max} of the ground, first, and second vibrational levels is compared with the maximum flux from any of the $v = 0$, $v = 1$, and $v = 2$ vibrational eigenstates (open symbols) in Figures 2a and 2b. The filled symbols denote the maximum flux obtainable using the optimized linear combination $\psi_1^{\text{max}}/\psi_2^{\text{max}}$ of the $v = 0$, $v = 1$, and $v = 2$ eigenstates. The circles represent the J_1 , and the triangles correspond to J_2 .

We can infer from Figure 2a that considerable total dissociation is seen for field amplitudes $0.003 \text{ au} \leq A \leq 0.01 \text{ au}$ ($19\text{--}65 \text{ TW/cm}^2$), but in this range there is an uniform increase in the dissociation out of both the channels and thus amplitude alone does not seem to be a suitable agent for enhanced selectivity. Also, for field amplitudes $A \leq 0.002 \text{ au}$ (13 TW/cm^2) the total dissociation is small and for $A \geq 0.006 \text{ au}$ (39 TW/cm^2) the dissociation is more or less complete whereby for $A \leq 0.002 \text{ au}$ and $A \geq 0.006 \text{ au}$ the extent of enhancement offered by the optimized linear combinations (filled symbols) is almost negligible as compared to the maximum flux that can be obtained with $v = 0$, $v = 1$, and $v = 2$ eigenstate as the

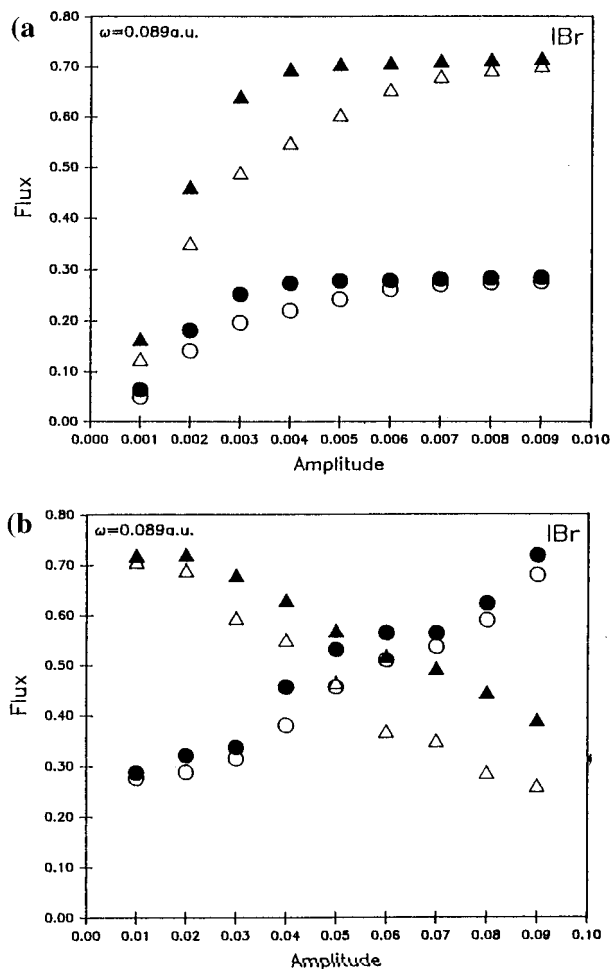


Figure 2. (a) Variation of maximum flux out of channel 1 [$I + \text{Br}(^2P_{3/2})$ (circles)] and channel 2 [$I + \text{Br}^*(^2P_{3/2})$ (triangles)] as a function of field amplitude A . The open symbols denote maximum flux from any of the three $v = 0$, $v = 1$, and $v = 2$ vibrational eigenstates, and the filled symbols represent those utilizing the channel specific optimized superposition of these states $\psi_1^{\text{max}}/\psi_2^{\text{max}}$. The results are for the three color CW field $\epsilon(t) = A \sum_{p=0}^2 \cos(\omega - \omega_{p,0})t$ with $\omega = 0.089$ au and amplitude range 0.001–0.009 au. (b) Same as in Figure 2a, but for the amplitude range 0.01–0.09 au.

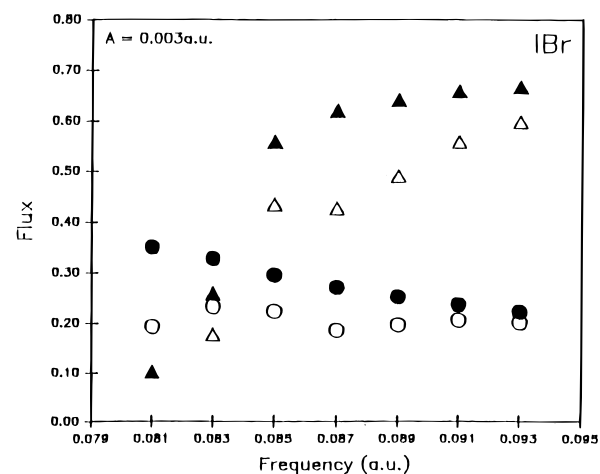


Figure 3. Variation of maximum flux with change in laser frequency at amplitude $A = 0.003 \text{ au}$. Conventions of Figure 2 apply.

initial condition (open symbol). As we approach larger field amplitudes (Figure 2b), the uniform increase of dissociation out of both the channels gives way to increased dissociation out of the $I + \text{Br}$ channel and decrease in the yield of $I + \text{Br}^*$, till at larger amplitudes the yield is predominantly out of the lower I

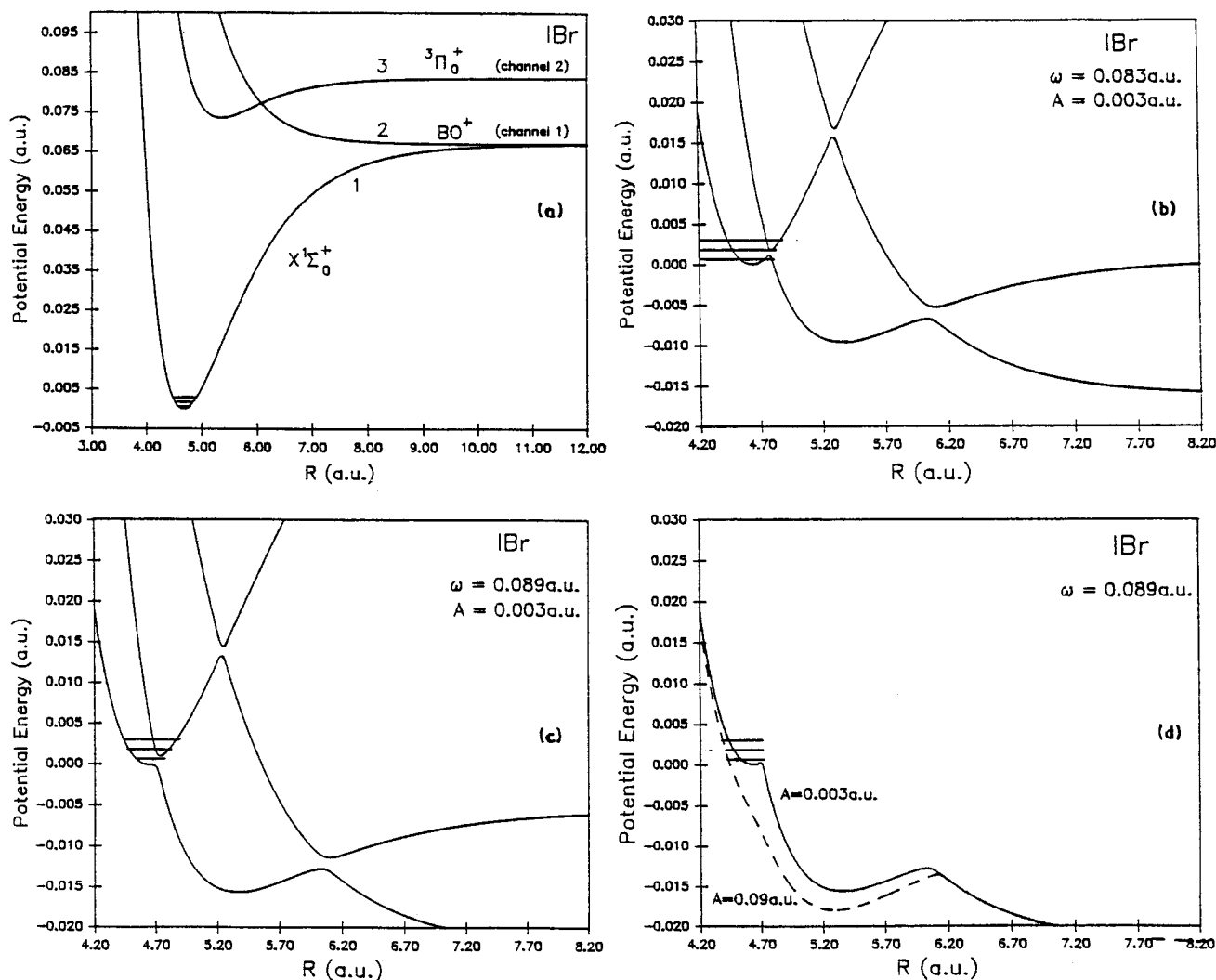


Figure 4. The field-free potential energy curves and the vibrational levels $v = 0$, $v = 1$, and $v = 2$ of IBr (a) and the dressed potential energy curves at $\omega = 0.083$ au, $A = 0.003$ au (b), $\omega = 0.089$ au, $A = 0.003$ au (c) and the dressed BO^+ state at $\omega = 0.089$ au and $A = 0.003$ au (solid line) and for same ω but $A = 0.09$ au (dashed line) (d).

+ Br channel. All these results for amplitude dependence are for $\omega = 0.089$ au chosen so that both the channels are asymptotically open.

It is experimentally advantageous to maintain as low an amplitude as possible and we explore the possibility of selective product enhancement at a comparatively low amplitude of $A = 0.003$ au (19 TW/cm²) by varying the field frequency. The results for the frequency band 0.081–0.093 au [17780–20410 cm⁻¹] are presented in Figure 3 where it can be seen that even at this low amplitude ($A = 0.003$ au), considerable selectivity and enhancement may be achieved by varying the field frequency. It is also seen that for extreme cases where there is less dissociation or where there is total dissociation, very little maximization is afforded by the optimized superposition of the linear combination, but away from these two extremes, considerable enhancement is seen as compared to the maximum available from a single initial condition.

This complementary role of amplitude and frequency variation can be understood by examining the change in the dressed electronic curves as a function of field variations. The field-free potential energy curves are plotted in Figure 4a, and the dressed adiabatic electron field curves²⁷ for different field parameters are presented in Figures 4b–d, where we see that in the presence of the field, even at low amplitude, the $v = 0$ level becomes unbound (Figure 4b) and the speed with which the molecule will approach the outermost crossing controlling

dissociation depends on field frequency (Figure 4c) with higher frequencies providing higher velocity diabatic approach to the $^3\Pi_0^+ - BO^+$ crossing, favoring exit out of the higher I + Br* channel. As the amplitude is increased (Figure 4d), the depth of the well to be traversed before approaching the crossing point increases leading to slower approach to the $^3\Pi_0^+ - BO^+$ crossing whereby exit out of the lower channel is favored as seen earlier in Figure 2b.

The results discussed so far were for the field form without any phase lag between the three colors. The results from phase variation between the three colors ω , $\omega - \omega_{10}$ and $\omega - \omega_{20}$ are collected in Table 1 where we can see that phase variations do not seem to be an effective tool for flux enhancement. In fact the effect of the phase lag is almost negligible for values considered here.

It is much easier to produce Gaussian pulses, and in Figure 5 we present the variation of the flux as a function of frequency for fluence normalized Gaussian pulses of the form

$$\epsilon(t) = A_{\text{norm}} \exp(-\alpha(t - t_0)^2) \sum_{p=0}^2 \cos(\omega - \omega_{p,0})t$$

where A_{norm} is adjusted so that for each ω the fluence delivered by the Gaussian pulse [$\alpha = 1.26 \times 10^{-7}$, $t_0 = 10000$ au (half the pulse length of the CW pulses considered earlier)] is the same

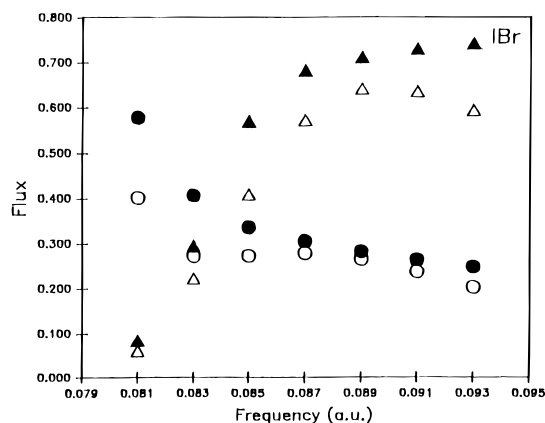


Figure 5. Same as Figure 3 but for a three-color fluenced normalized Gaussian field $\epsilon(t) = A_{\text{norm}} \exp(-\alpha(t - t_0)^2) \sum_{p=0}^2 \cos(\omega - \omega_{p,0})t$ where $\alpha = 1.26 \times 10^{-7}$, $t_0 = 10000$ au (half the CW pulse length) and A_{norm} is adjusted to deliver the same fluence as the CW field with $A = 0.003$ au used earlier. Conventions of Figure 2 apply.

TABLE 1: Maximum Flux Out of I + Br and I + Br* Channels with and without Optimization of the Initial State as a Function of Phase Variations for the Photolysis Field $\epsilon(t) = A[\cos(\omega t) + \cos((\omega - \omega_{1,0})t + \delta_1) + \cos((\omega - \omega_{2,0})t + \delta_2)]$

δ_1	δ_2	channel 1		channel 2	
		max. unopt flux	max. opt flux	max. unopt flux	max. opt flux
0	0	0.196	0.252	0.490	0.641
0	$\pi/4$	0.199	0.252	0.498	0.641
0	$\pi/2$	0.215	0.251	0.538	0.638
0	$3\pi/4$	0.230	0.248	0.577	0.629
0	p	0.236	0.245	0.591	0.620
$\pi/4$	0	0.218	0.247	0.545	0.630
$\pi/4$	$\pi/4$	0.202	0.252	0.504	0.644
$\pi/4$	$\pi/2$	0.195	0.255	0.488	0.652
$\pi/4$	$3\pi/4$	0.203	0.256	0.508	0.652
$\pi/4$	p	0.217	0.252	0.542	0.642

as that from the CW field with $A = 0.003$ au used earlier. The trend of flux maximization is similar to that from the corresponding CW pulse, but the yield using Gaussian pulses are greater. Gaussian pulses may therefore be employed to achieve equally effective selective control with enhanced product yield.

IV. Concluding Remarks

In this paper we have offered an investigation of selective maximization of IBr photodissociation products using Rayleigh–Ritz variational optimization procedure for the flux operator. Optimization increases the product yield out of both the channels, and our results demonstrate that a careful choice of field parameters in conjunction with the variationally optimized initial state can deliver almost any desired Br*/Br ratio. Similar selectivity has been demonstrated earlier using the coherent control approach²⁰ which, however, is perturbation theoretic. The optimal control approach applied to this problem²¹ also achieved large flux and almost total selectivity but required three orders of magnitude more intense fields.

The approach advocated here therefore offers the possibility of obtaining controlled selective dissociation resulting in

substantial yields using moderate intensity lasers. The selective flux maximization procedure outlined here is equally effective with the CW or Gaussian pulses, offering additional experimental convenience and flexibility. The preparation of the optimal initial linear combination however requires overtone excitation using a two color ($\omega_{10} + \omega_{20}$) IR laser. The field required to achieve the requisite $\{c_m^{\text{max}}\}_{m=0}^2$ values may be obtained analytically for the three vibrational levels¹³ or the more general Optimal Control Theory⁹ may also be applied to this task. A scheme based on the Parametric Equations of Motion to obtain the desired population mix by investigating population dynamics as a function of field parameters has been applied to HF^{18,28} and could be profitably employed here as well. At this stage of development, however, what would serve the purpose better is an experimental test of the ideas presented here, and hopefully the detailed demonstration of its promise will stimulate some experimental investigations.

Acknowledgment. M.K.M. acknowledges financial support from the BRNS (Grant No. BRNS 37/9/94-R & D-II/787) of the DAE. D.B.B. acknowledges the support from CSIR, India (SRF Fellowship Grant No. 9/87(143) 92/EMR-I).

References and Notes

- (1) Crim, F. F. *Science* **1990**, *249*, 1387.
- (2) Rice, S. A. *Science* **1992**, *258*, 412.
- (3) Warren, W. A.; Rabitz, H. A.; Dahleh, M. *Science* **1993**, *259*, 1581.
- (4) Shapiro, M.; Brumer, P. *Int. Rev. Phys. Chem.* **1994**, *13*, 187.
- (5) Brumer, P.; Shapiro, M. *Annu. Rev. Phys. Chem.* **1992**, *43*, 257.
- (6) Tannor, D. J.; Rice, S. A. *J. Chem Phys.* **1985**, *83*, 5013.
- (7) Jiang, X.; Shapiro, M.; Brumer, P. *J. Chem. Phys.* **1996**, *104*, 607.
- (8) Chen, Z.; Brumer, P.; Shapiro, M. *J. Chem. Phys.* **1993**, *98*, 6843.
- (9) Shi, S.; Rabitz, H. *Chem. Phys.* **1989**, *139*, 185. (b) Shi, S.; Woody, A.; Rabitz, H. *J. Chem. Phys.* **1990**, *92*, 2927.
- (10) Tannor, D. J.; Kosloff, R.; Rice, S. A. *J. Chem Phys.* **1986**, *85*, 5805.
- (11) Kosloff, R.; Rice, S. A.; Gaspard, P.; Tersigni, S.; Tannor, D. J. *Chem. Phys.* **1989**, *139*, 201.
- (12) Tang, H.; Kosloff, R.; Rice, S. A. *J. Chem. Phys.* **1996**, *104*, 5457.
- (13) Gross, P.; Gupta, A. K.; Bairagi, D. B.; Mishra, M. K. *J. Chem. Phys.* **1996**, *104*, 7045.
- (14) Kalyanaraman, C.; Sathyamurthy, N. *Chem. Phys. Lett.* **1993**, *209*, 52.
- (15) Zhu, L.; Kleiman, V.; Li, X.; Lu, S. P.; Trentelman, K.; Gordon, R. J. *Science* **1995**, *270*, 77.
- (16) Park, S. M.; Lu, S. P.; Gordon, R. J. *J. Chem. Phys.* **1991**, *94*, 8622. (b) Lu, S. P.; Park, S. M.; Xie, Y.; Gordon, R. J. *J. Chem. Phys.* **1992**, *96*, 6613.
- (17) Imre, D. G.; Zhang, J. *Chem. Phys.* **1989**, *139*, 89. (b) Vander Wal, R. L.; Scott, J. L.; Crim, F. F.; Weide, K.; Schinke, R. *J. Chem. Phys.* **1991**, *94*, 3548. (c) Crim, F. F. *Annu. Rev. Phys. Chem.* **1993**, *44*, 397. (d) Cohen, Y.; Bar, I.; Rosenwaks, S. *J. Chem. Phys.* **1995**, *102*, 3612.
- (18) Gupta, A. K.; Gross, P.; Bairagi, D. B.; Mishra, M. K. *Chem. Phys. Lett.* **1996**, *257*, 658.
- (19) Devries, M. S.; van Veen, M. J. A.; DeVries, A. E. *Chem. Phys. Lett.* **1978**, *56*, 15. (b) Devries, M. S.; van Veen, M. J. A.; DeVries, A. E. *Chem. Phys. Letts.* **1980**, *51*, 159.
- (20) Chan, C. K.; Brumer, P.; Shapiro, M. *J. Chem. Phys.* **1991**, *94*, 2688.
- (21) Gross, P.; Bairagi, D. B.; Mishra, M. K.; Rabitz, H. *Chem. Phys. Lett.* **1994**, *223*, 263.
- (22) Alexander, M.; Pouilly, B.; Duhoo, T. *J. Chem. Phys.* **1993**, *99*, 1752.
- (23) Marston, C. C.; Balint-Kurti, G. G. *J. Chem. Phys.* **1989**, *91*, 3571.
- (24) Feit, M. D.; Fleck, J. A. *J. Chem. Phys.* **1984**, *80*, 2578.
- (25) Kosloff, R. *J. Phys. Chem.* **1988**, *92*, 2087.
- (26) Gross, P.; Neuhauser, D.; Rabitz, H. *J. Chem. Phys.* **1992**, *96*, 2834.
- (27) George, T. F. *J. Phys. Chem.* **1982**, *86*, 10.
- (28) Gross, P.; Gupta, A. K.; Bairagi, D. B.; Mishra, M. K. *Chem. Phys. Lett.* **1995**, *236*, 8.